Derivation of an Evolution Equation for Two-Dimensional Waves on Thin Films

Randall J.T. Goodnight

Thesis submitted to the Faculty of the
Virginia Polytechnic Institute and State University
in partial fulfillment of the requirements for the degree of

Master of Science
in
Engineering Mechanics

Mark S. Cramer, Chair
Sungwhun Jung
Saad A. Ragab

May 6, 2013
Blacksburg, Virginia

Keywords: Thin Films, Undercompressive Shock, Non-Convex Flux, Marangoni Stress, Surface Tension

Derivation of an Evolution Equation for Two-Dimensional Waves on Thin Films

Randall J.T. Goodnight

We examine wave propagation on thin liquid films subjected to gravity, fluid friction, surface tension, and Marangoni effects. The physical configuration is a thin liquid layer on a planar incline. Following previous studies, the Marangoni effect is incorporated by a constant surface tension gradient and yields a non-convex flux function in our thin film equation. We extend previous studies by deriving the thin film equation governing two-dimensional waves on the liquid layer. We then derive a simplified evolution equation governing weakly nonlinear, quasi-planar, and weakly dissipative waves on the layer. When the undisturbed state is in the vicinity of an inflection point in the streamwise component of the flux function, the mixed nonlinearity, fourth order dissipation and the transverse modulations interact over time scales on the order of the scaled amplitude to the negative second power. The effect the transverse modulations is found to be intrinsically nonlinear.

Contents

List of Figures

Chapter 1

Introduction

Wave propagation in thin films has been a topic of interest in many recent studies. Applications include industrial coating, spin coating, thin film heat exchangers, painting, cooling towers, wetted columns, and applications involving aircraft de-icing; see, e.g., references [1], [2], [3], [5], [10], and [12]. Of direct interest to the present work is that of Bertozzi, et al [2] who examined a two-dimensional thin film driven by gravity and Marangoni effects. The primary focus of Bertozzi, et al was to describe the highly non-classical wave propagation possible in systems having a non-convex flux function combined with a fourth order dissipation term. Using a simplification of the thin film equation, they showed that such a system admits undercompressive shock waves. Undercompressive shocks are those which violate the Lax speed-ordering relation [6]. As discussed in Appendix C, the speed-ordering condition requires that the shock speed be less than or equal to the wave speed behind it and greater than or equal to the wave speed ahead of it. Thus, such undercompressive shocks would seem to violate causality and are of general interest in the more general field of nonlinear wave propagation.

The model equation employed by Bertozzi, et al [2] described one-dimensional waves only. The main objective of the present study is to extend Bertozzi et als equation from one to two dimensions. We derive a relatively simple form of the thin film equation which contains a non-convex flux function, a simple fourth order dissipation and accounts for long transverse modulations. Although the present study is entirely analytical in nature, we expect that numerical solutions of our evolution equation can be used to determine the likelihood of observing undercompressive shocks on thin films in the laboratory where there are always transverse perturbations which may or may not modify the already sensitive undercompressive shocks. It may also turn out that the transverse modulations can focus or de-focus resulting in a transition from the regime admitting classical shock waves to that admitting undercompressive shocks.

We begin by deriving a two-dimensional version of Bertozzi et als [2] thin film equation. In order to generate a non-convex flux, Bertozzi et al have ignored surface tension gradients

except for an imposed gradient for which the surface tension varied in the direction of the main flow. The length scale over which the surface tension varied was taken to be much larger than the wavelengths and other natural scales of the problem. Thus, the surface tension gradient was taken to be a constant. A constant surface tension gradient, like the one used in this thesis, could be realized with a strong thermally induced surface tension gradient. In the present study we impose this condition of a constant surface tension gradient. Other milder assumptions made here and in [2] include the condition that the solid surface is prewetted so that contact line effects can be ignored. We note that other authors have considered two dimensional films. Edmonstone [4] has derived a system of equations governing thin film waves with no externally imposed surface tension gradient. The variation of surface tension was due to variations of surfactant concentrations generated by stretching of the surface due to the wave disturbances themselves. The nonlinearity was seen to generate a convex flux function and the dissipation was seen to be of second rather than fourth order. Thus, the scales considered by Edmonstone [4] will not generate undercompressive shocks. Myers [7] also developed a two dimensional thin film model, however Myers model was focused upon the analysis of solidification of a thin film on an arbitrary surface and did not consider surface tension as a driving force.

We have also found that the derivations given by the previous authors frequently used results without proof and questions naturally arose as to whether the approximations used were self-consistent. We have therefore derived the basic two-dimensional version of Bertozzi et als equation from first principles. Thus, in Chapter 2 we state our exact Navier Stokes equations, the corresponding boundary conditions, the physical problem to be examined, and the scalings to be applied. In Chapter 3 we approximate the exact Navier Stokes equations to obtain the extension of the equation considered in [2]. In Chapter 4 we then derive a simplified evolution equation which contains a non-convex nonlinearity, a relatively simple fourth order dissipation and the effects of gradual transverse modulations simplified. In Chapter 5, we also establish an analogous equation for problems involving convex nonlinearity.

Chapter 2

Formulation

As discussed in Section 1, we will consider essentially the same physical configuration as described by Bertozzi et al. [2]. An incompressible thin film is driven up a pre-wetted plane inclined at angle θ to the horizontal by the effects of gravity and a thermally induced surface tension gradient. The height of the film, $h = h(x, y, t)$, will be measured normal to the plane as shown in Figure 2.1. The plane is taken to be pre-wetted to minimize complications arising from the paradox of a flow of infinitesimal thickness at the leading edge of the film when the no slip condition is considered.

The fundamental equations used to describe the flow in this thesis are the incompressible continuity equation,

$$u_x + v_y + w_z = 0 \tag{2.1}$$

where u, v, and w denote the velocity components in the x, y, and z directions respectively and a subscript of x, y, or z denotes a derivative with respect to the subscript variable, and the Navier Stokes equation. Throughout this thesis, a subscript of x, y, z, or t will refer to a partial derivative with respect to the subscript variable. The Navier Stokes equation in the x direction is

$$\rho\frac{Du}{Dt} + P_x = \mu(u_{yy} + u_{xx} + u_{zz}) + \rho g\sin(\theta) \tag{2.2}$$

where $\frac{D}{Dt}$ denotes the material derivative, P_x is the derivative of pressure with respect to x, μ is the dynamic viscosity, ρ is the density of the fluid, g is the acceleration of gravity, and θ is the constant angle of the incline.

In the y direction the Navier Stokes equation is

$$\rho\frac{Dv}{Dt} + P_y = \mu(v_{yy} + v_{xx} + v_{zz}), \tag{2.3}$$

and, in the z direction the Navier Stokes equation is

$$\rho\frac{Dw}{Dt} + P_z = \mu(w_{yy} + w_{xx} + w_{zz}) - \rho g\cos(\theta). \tag{2.4}$$

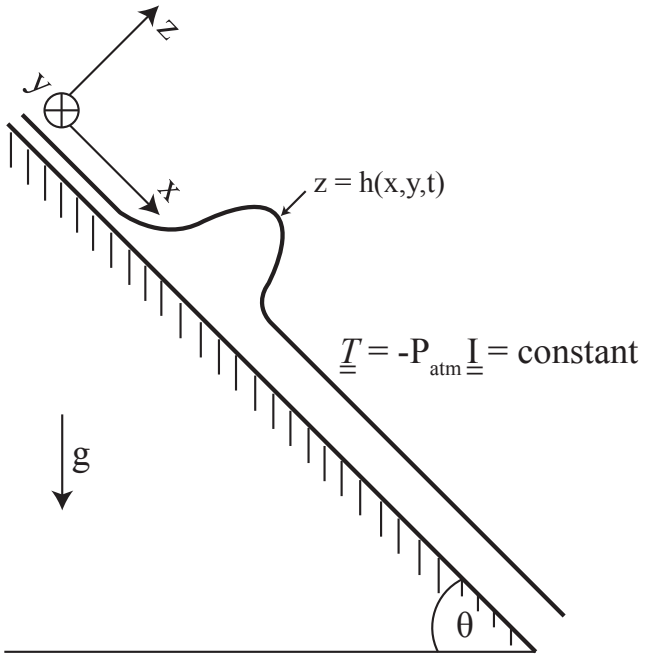

Figure 2.1: Thin film flow on inclined plane. Here P_{atm} is the constant atmospheric pressure, $\underline{\underline{I}}$ is the identity matrix, and $\underline{\underline{T}}$ is the total stress tensor.

The boundary conditions that will be used are the no slip condition, where all velocity components at the solid boundary of the plane must be zero, the kinematic boundary condition, which requires that there is no flux across the free surface of the fluid. The final boundary condition is the dynamic boundary condition, which states that the change in stress across the free surface must be balanced by the surface tension. The no slip condition is given by

$$u = v = w = 0 \tag{2.5}$$

at $z = 0$. The kinematic boundary condition can be written

$$h_t + uh_x + vh_y = w \tag{2.6}$$

at $z = h(x, y, t)$. The dynamic boundary condition can be written

$$\mathbf{n}(P - P_{atm}) - \mathbf{T}^T\mathbf{n} = -2\sigma H\mathbf{n} - \mathbf{T}_\alpha a^{\alpha\beta}\frac{\partial\sigma}{\partial u^\beta}. \tag{2.7}$$

where a Greek subscript or superscript denotes an index of 1 or 2 and a Latin subscript denotes an index of 1, 2, or 3. We employ the Einstein Summation Convention for both Greek and Latin indices. The form of Equation (2.7) comes from personal communication with M.S.Cramer, September 27, 2012. In Equation (2.7) the viscous part of the stress tensor is defined as

$$\mathbf{T} \equiv \mu \begin{bmatrix} 2u_x & u_y + v_x & u_z + w_x \\ u_y + v_x & 2v_y & v_z + w_y \\ u_z + w_x & v_z + w_y & 2w_z \end{bmatrix}. \tag{2.8}$$

If we employ a Gaussian representation for the surface, we may write the unit vector normal to the surface as

$$\mathbf{n} \equiv \frac{\boldsymbol{\epsilon}_3 - h_x\boldsymbol{\epsilon}_1 - h_y\boldsymbol{\epsilon}_2}{(1+h_x^2+h_y^2)^{1/2}}. \tag{2.9}$$

Here $\boldsymbol{\epsilon_1}$, $\boldsymbol{\epsilon_2}$, $\boldsymbol{\epsilon_3}$ represent the unit base vectors in the x, y, and z directions, respectively. In (2.7) the quantity σ is the surface tension and H denotes the mean curvature of the $z = h(x, y, t)$ surface which can be written as

$$H \equiv \frac{(1+h_y^2)h_{xx} + (1+h_x^2)h_{yy} - 2h_xh_yh_{xy}}{2(1+h_x^2+h_y^2)^{3/2}}. \tag{2.10}$$

The surface base vectors, $\mathbf{T}_\alpha$, are defined through a relation to the cartesian coordinates, $z^i \equiv (x, y, h(x, y, t))$, and cartesian base vectors, $\boldsymbol{\epsilon}_i$ as follows:

$$\mathbf{T}_\alpha \equiv \frac{dz^i}{du^\alpha}\boldsymbol{\epsilon}_i, \tag{2.11}$$

where, for the Gaussian representation of the surface, we may take $u^1 = x$ and $u^2 = y$. The quantity $a^{\alpha\beta}$ is the inverse of the surface metric $a_{\alpha\beta}$ defined as

$$a_{\alpha\beta} \equiv \mathbf{T}_\alpha \cdot \mathbf{T}_\beta = \begin{bmatrix} 1+h_x^2 & h_xh_y \\ h_xh_y & 1+h_y^2 \end{bmatrix}, \tag{2.12}$$

i.e.

$$a^{\alpha\beta} = \frac{1}{1+h_x^2+h_y^2}\begin{bmatrix} 1+h_y^2 & -h_xh_y \\ -h_xh_y & 1+h_x^2 \end{bmatrix}. \tag{2.13}$$

The explicit form of the last term in equation (2.7) is found by expansion of equation (2.11) and use of Equation(2.13) to yield

$$\mathbf{T}_\alpha a^{\alpha\beta}\frac{\partial\sigma}{\partial u^\beta} = \frac{\sigma_x}{A}(C\boldsymbol{\epsilon}_1 - h_xh_y\boldsymbol{\epsilon}_2 + h_x\boldsymbol{\epsilon}_3) + \frac{\sigma_y}{A}(-h_xh_y\boldsymbol{\epsilon}_1 + D\boldsymbol{\epsilon}_2 + h_y\boldsymbol{\epsilon}_3) \tag{2.14}$$

where $A = 1 + h_x^2 + h_y^2$, $C = 1 + h_y^2$ and $D = 1 + h_x^2$.

In equation (2.7) the first term, $\mathbf{n}(P - P_{atm})$, is recognized as the difference in pressure between the liquid and the surrounding air. The second term, $\mathbf{T}^T\mathbf{n}$ is the measure of the viscous stresses in the fluid. The first term on the right hand side of equation (2.7) is the conventional surface tension term proportional to the mean curvature. Were the surface a plane the curvature would be zero and this term would vanish from the equation. The last term, $\mathbf{T}_\alpha a^{\alpha\beta}\frac{d\sigma}{du^\beta}$ is due to variations of the surface tension along the surface and is called the Marangoni stress. In order to simplify the application of the dynamic boundary condition, it is convenient to separate (2.7) into x, y and z directions. The result is

$$-(P - P_{atm})h_x - (-h_xT_{11} - h_yT_{12} + T_{13}) = h_x\sigma 2H - \sigma_x\frac{C}{A^{1/2}} + \sigma_y\frac{h_xh_y}{A^{1/2}} \tag{2.15}$$

in the x direction. In the y direction we have

$$-(P - P_{atm})h_y - (-h_x T_{21} - h_y T_{22} + T_{23}) = h_y \sigma 2H + \sigma_x \frac{h_x h_y}{A^{1/2}} - \sigma_y \frac{D}{A^{1/2}} \tag{2.16}$$

and, in the z direction

$$(P - P_{atm}) - (-h_x T_{31} - h_y T_{32} + T_{33}) = -\sigma 2H - \sigma_x \frac{h_x}{A^{1/2}} - \sigma_y \frac{h_y}{A^{1/2}}, \tag{2.17}$$

where T_{ij} are the components of the stress tensor (2.8). Solving equations (2.15) through (2.17) for $(P - P_{atm})$, it can be seen that

$$P - P_{atm} = \frac{-\sigma}{A^{3/2}}(Ch_{xx} + Dh_{yy} - 2h_y h_x h_{xy}) - \frac{2\sigma_x h_x}{A^{1/2}(2 - A)} - \frac{2\sigma_y h_y}{A^{1/2}(2 - A)} \tag{2.18}$$

at $z = h$.

The flows if interest will all be variants of the steady, two-dimensional, fully developed flow of the liquid down the incline of Figure 2.1. This base flow will be taken to correspond to a liquid layer of constant thickness of order h_0 and a constant surface tension. The well-known solution to this problem yields a mass flux per unit distance into the page of

$$\dot{m} = \frac{\rho^2 g \sin\theta}{3\mu} h_0^3, \tag{2.19}$$

where for now we take the thickness of the film to be h_0. Thus the average velocity can be defined

$$U = \frac{\rho g \sin\theta}{3\mu} h_0^2. \tag{2.20}$$

In all that follows, we take $\sin\theta = O(1)$, i.e. $\theta \not\approx 0$, and we may therefore regard

$$u, v = O(U) = O\left(\frac{\rho g}{\mu} h_0^2\right). \tag{2.21}$$

We now consider the scales for the perturbed flow. The perturbation to the free interface will be taken to have length L such that

$$\frac{\partial}{\partial x}, \frac{\partial}{\partial y} = O\left(\frac{1}{L}\right), \tag{2.22}$$

and

$$\frac{\partial}{\partial z} = O\left(\frac{1}{h_0}\right). \tag{2.23}$$

If we also take the velocities in the transverse direction we can use (2.1) to deduce that

$$w = O\left(\frac{h_0}{L} U\right). \tag{2.24}$$

Although there is no simple apriori way to deduce the size of the pressure perturbation caused by the disturbance to our base flow, we note that the analysis of Chapter 4 will require that the pressure be scaled with the viscous scale, such that

$$\Delta P = O\left(\frac{\mu L U}{h_0^2}\right). \tag{2.25}$$

In all that follows, we will take the layer to be thin such that

$$\frac{h_0}{L} << 1, \tag{2.26}$$

as in the lubrication theory approximations of [9] and [11]. Furthermore, we make the slow flow or lubrication approximation which requires that

$$\frac{Re h_0^2}{L^2} << 1 \tag{2.27}$$

where $Re \equiv \frac{UL\rho}{\mu}$, where $\nu \equiv \frac{\mu}{\rho}$ is the kinematic viscosity of the fluid. These two restrictions will be used to reduce the Navier Stokes equations.

In addition to lubrication theory assumptions, we follow Bertozzi et al [2] in taking the surface tension gradient to be constant. The size of the surface tension is determined from the size of the pressure and is

$$\sigma = O\left(\frac{\Delta P L^2}{h_0}\right) = O\left(\frac{U\mu L^3}{h_0^3}\right). \tag{2.28}$$

If we write the Weber number in terms of surface tension, we can see

$$We = \frac{L\rho U^2}{\sigma} = O\left(\frac{Re h_0^3}{L^3}\right) << 1. \tag{2.29}$$

Physically the condition of a constant surface tension gradient could be realized by imposing a strong thermal gradient. The surface tension gradient that results from this thermal input varies over a scale, $\mathcal{L}$, greater than the characteristic length of the wave fronts L such that

$$\frac{L}{\mathcal{L}} << 1. \tag{2.30}$$

With this in mind, the surface tension gradient is taken to be a constant. This assumption will allow the work of this thesis to extend naturally from the work of Bertozzi et al [2], as the surface tension gradient was also taken to be constant in [2]. Including the length scale of variations in surface tension, partial derivatives of the surface tension with respect to x or y will be defined as

$$\frac{\partial \sigma}{\partial x} = \frac{\partial \sigma}{\partial y} = O\left(\frac{\sigma}{\mathcal{L}}\right). \tag{2.31}$$

Chapter 3

Thin Film Equation

We now use the approximations of Chapter 2 to derive the two dimensional thin film equation. We first consider the x component of the Navier Stokes equation (2.2). First the material derivative is weighed against the second derivative of u with respect to z. Taking the orders of the result, we have

$$\frac{\rho\frac{Du}{Dt}}{\mu u_{zz}} = O\left(\frac{\rho\frac{U^2}{L}}{\mu\frac{U}{h_0^2}}\right), \tag{3.1}$$

where we take

$$\frac{D}{Dt} = O\left(\frac{U}{L}\right). \tag{3.2}$$

After simplification, the result is

$$\frac{\rho\frac{Du}{Dt}}{\mu u_{zz}} = O\left(Re\frac{h_0^2}{L^2}\right). \tag{3.3}$$

The lubrication theory approximation given by (2.27), requires that is be small. Thus, the material derivative can be neglected compared to the largest viscous term. In a similar manner, the second derivative of u with respect to x is weighed against the second derivative of u with respect to z. The result is

$$\frac{u_{xx}}{u_{zz}} = \left(\frac{h_0^2}{L^2}\right) << 1, \tag{3.4}$$

from (2.26). Similarly, the second derivative of u with respect to y can be seen to be negligible compared to u_{zz}. The reduced Navier Stokes equation in the x direction then reduces to

$$P_x \approx \mu u_{zz} + \rho g \sin(\theta). \tag{3.5}$$

The motivation for (2.25) should now be clear. That is, it is required in order to ensure that the pressure forces are of the same size as the friction forces. In like manner (2.3) can be reduced to

$$P_y \approx \mu v_{zz}. \tag{3.6}$$

Reduction of (2.4) is possible through similar approximations. First the material derivative is weighed against P_z. If we take the ratio of the inertia and pressure forces, we find

$$\frac{\rho\frac{Dw}{Dt}}{P_z} = O\left(\frac{\rho\frac{U^2 h_0}{L^2}}{\frac{\Delta P}{h_0}}\right). \tag{3.7}$$

After simplification, the result is

$$\frac{\rho\frac{Dw}{Dt}}{P_z} = O\left(Re\frac{h_0^4}{L^4}\right). \tag{3.8}$$

Again, the material derivative is seen to be small in comparison to the change in pressure term in the Navier Stokes equation leading to a reduced equation of the form:

$$P_z \approx \mu(w_{xx} + w_{yy}) - \rho g\cos(\theta). \tag{3.9}$$

Further reduction of equation (3.9) is possible through observing

$$\frac{\mu(w_{xx} + w_{yy})}{P_z} = O\left(\frac{\frac{\mu U h_0}{h_0^2 L}}{\frac{\Delta P}{h_0}}\right). \tag{3.10}$$

If we use (2.25), (3.10) can be reduced to

$$\frac{\mu(w_{xx} + w_{yy})}{P_z} = O\left(\frac{h_0^2}{L^2}\right) << 1 \tag{3.11}$$

by (2.26). The viscous term of (3.9) can thus been seen to be negligible compared to the pressure term and (3.9) can be reduced to

$$P_z \approx -\rho g\cos(\theta). \tag{3.12}$$

An additional order of magnitude analysis of the stress tensor (detailed in Appendix A) reveals that (2.8) can be approximated as:

$$\mathbf{T} \approx \mu\begin{bmatrix} 2u_x & u_y + v_x & \sigma_x \\ u_y + v_x & 2v_y & \sigma_y \\ \sigma_x & \sigma_y & 2w_z \end{bmatrix}. \tag{3.13}$$

If we now integrate (3.12) we find

$$P - P_{atm} = -\rho g z \cos(\theta) + g_1, \tag{3.14}$$

where $g_1 = g_1(x, y, t)$. If we combine (3.14) with (2.18) we can determine g_1. When this is done, the resultant expression for (3.14) is

$$P - P_{atm} \approx -\rho g \cos(\theta)(z - h) + F, \tag{3.15}$$

where

$$F \equiv -\frac{\sigma}{A^{3/2}}(Ch_{xx} + Dh_{yy} - 2h_x h_y h_{xy}) - \frac{2}{A^{1/2}(2 - A)}(\sigma_x h_x + \sigma_y h_y). \tag{3.16}$$

If we differentiate (3.15) with respect to x and substitute the result into (3.5) we find that

$$\mu u_{zz} \approx \rho g[\cos(\theta)h_x - \sin(\theta)] + F_x. \tag{3.17}$$

A single integration of (3.17) with respect to z results in

$$\mu u_z \approx [\rho g(\cos(\theta)h_x - \sin(\theta)) + F_x]z + g_2 \tag{3.18}$$

where $g_2 = g_2(x, y, t)$ and can be found through use of the boundary condition (2.7). If we use the approximations of the viscous stress tensor detailed in Appendix A we have $\mu u_z = \sigma_x$ at $z = h$. Thus, (3.18) becomes

$$\mu u_z \approx [\rho g(\cos(\theta)h_x - \sin(\theta)) + F_x](z - h) + \sigma_x \tag{3.19}$$

and, after a second integration and use of (2.5), u is found to be

$$u \approx \frac{1}{\mu}(\rho g(\cos(\theta)h_x - \sin(\theta)) + F_x)(\frac{z^2}{2} - hz) + \sigma_x z. \tag{3.20}$$

In a similar manner, (3.15) can be differentiated with respect to y and combined with (3.6). Double integration then yields

$$v \approx \frac{1}{\mu}(\rho g \cos(\theta h_y) + F_y)(\frac{z^2}{2} - hz) + \sigma_y z. \tag{3.21}$$

Equations (3.20)-(3.21) can then be substituted in (2.1), i.e., in

$$w_z = -(u_x + v_y). \tag{3.22}$$

Carrying out the integration with respect to z, w is seen to be

$$\begin{aligned} w \approx \frac{-1}{\mu}[(\frac{h^3}{6} - \frac{zh^2}{2})(\rho g \cos(\theta)h_{xx} + F_{xx} + \rho g \cos(\theta)h_{yy} + F_{yy}) \\ + \frac{z^2}{2}(-h_y(\rho g \cos(\theta)h_y + F_y) \\ -h_x(\rho g(\cos(\theta)h_x - \sin(\theta)) + F_x))]. \end{aligned} \tag{3.23}$$

Substitution of (3.20), (3.21), and (3.23) into (2.6), yields

$$h_t \approx \frac{1}{\mu}[(\frac{h^3}{3}G)_y + (\frac{h^3}{3}J)_x - (\frac{h^2}{2}\sigma_y)_y - (\frac{h^2}{2}\sigma_x)_x] \tag{3.24}$$

where

$$G = \rho g \cos(\theta) h_y + F_y \tag{3.25}$$

and

$$J = \rho g[\cos(\theta)h_x - \sin(\theta)] + F_x. \tag{3.26}$$

Further simplification of (3.24)-(3.26) can be accomplished through further use of the ordering detailed in Chapter 2. First, it can be seen from the lubrication approximations (2.26)-(2.27) that A, C, and D are all approximately one. Second, when the sine and cosine terms of J and G are weighed against each other, it is seen that with the coefficient of h_x or h_y the cosine term will always be smaller. As pointed out in Chapter 2, θ will never approach zero, therefore $\sin(\theta)$ will never be small. Equations (3.24)-(3.26) become

$$h_t \approx \frac{1}{\mu}[(\frac{h^3}{3}F_y)_y + (\frac{h^3}{3}(-\rho g(\sin(\theta)) + F_x))_x - (\frac{h^2}{2}\sigma_y)_y - (\frac{h^2}{2}\sigma_x)_x] \tag{3.27}$$

while F is now reduced to

$$F = -\sigma(h_{xx} + h_{yy} - 2h_x h_y h_{xy}) - 2(\sigma_x h_x + \sigma_y h_y). \tag{3.28}$$

Because h_x and h_y are small, the third term on the right hand side of (3.28) is much smaller than the first and second terms. Thus, F can be further reduced to

$$F = -\sigma(h_{xx} + h_{yy}) - 2(\sigma_x h_x + \sigma_y h_y). \tag{3.29}$$

Further reduction of F is possible through analysis of the scalings of the remaining terms. Weighing terms,

$$\frac{\sigma_x h_x}{\sigma h_{xx}} = O\left(\frac{\frac{\sigma h}{\mathcal{L}L}}{\frac{\sigma h}{L^2}}\right) = O\left(\frac{L}{\mathcal{L}}\right) << 1 \tag{3.30}$$

from (2.30).

Thus F is now seen to be

$$F \approx -\sigma(h_{xx} + h_{yy}). \tag{3.31}$$

Application of this form of F to the reduced (3.27) results in

$$\begin{aligned} h_t + \frac{\rho g \sin(\theta)}{3\mu}(h^3)_x + (\frac{h^2}{2\mu}\sigma_y)_y + (\frac{h^2}{2\mu}\sigma_x)_x \approx \\ -\frac{\sigma}{3\mu}[(h^3(h_{xxx} + h_{yyx}))_x + (h^3(h_{xxy} + h_{yyy}))_y] \end{aligned} \tag{3.32}$$

which is the desired extension of Bertozzi, et al's [2] one dimensional thin film equation. Here, no ad hoc conditions were needed to eliminate the second order diffusion. The equation holds for $\sigma_x > 0$ and $\sigma_x < 0$. As discussed in Appendix C, the former case results in a convex flux function and the latter case results in a non-convex flux function. Overall, the flux in the x direction is due to gravity, the surface tension gradient, and the $(h_{xx} + h_{yy})_x$ surface tension terms. The flux in the transverse or y direction is due only to the gradient of σ in the transverse direction and the surface tension. Wave propagation in the transverse direction will always involve a convex flux function and will therefore be classical. If we consider propagation in the x direction only, we recover equation (8) of [2], which is just a cubic Burgers equation combined with the Landau-Levich fourth order dissipation term. If we formally ignore gravity, we obtain a quadratic Burgers equation combined with the fourth order dissipation. As discussed in Appendices B and C, (3.32) can be classified as anisotropic (with respect to wave propagation), dispersive, and non-convex.

The form of (3.27) is in a simple conservative form which is easy to use in computational studies. However, in analytical studies, (3.27) is somewhat awkward due to the nonlinear terms in the dissipative terms. In fact, in [2], the dissipative term was simply represented as a term proportional to h_{xxxx}, i.e., the dissipative term was linearized. In the following chapter we follow [2] in seeking a self-consistent evolution equation which contains the important physical effects leading to undercompressive shocks and which also accounts for weak transverse modulations.

Chapter 4

Evolution of Quasi-Planar Wave Fronts

We will now take (3.32) to be exact for the purposes of studying the stability of the wave fronts. We now rewrite (3.32) in a more convenient form,

$$h_t + \mathcal{F}_x + \mathcal{G}_y = -\frac{\sigma}{3\mu}[(h^3(h_{xxx} + h_{yyx}))_x + (h^3(h_{xxy} + h_{yyy}))_y], \tag{4.1}$$

or

$$h_t + \mathcal{F}'(h)h_x + \mathcal{G}'(h)h_y = -\frac{\sigma}{3\mu}[(h^3(h_{xxx} + h_{yyx}))_x + (h^3(h_{xxy} + h_{yyy}))_y] \tag{4.2}$$

where

$$\mathcal{F}(h) = \frac{\rho g \sin(\theta)}{3\mu}h^3 + \frac{h^2}{2\mu}\sigma_x \tag{4.3}$$

and

$$\mathcal{G}(h) = \frac{h^2}{2\mu}\sigma_y. \tag{4.4}$$

Here a prime will denote a derivative with respect to h and h_0 will now be taken to be the undisturbed height of the film. Henceforth a function evaluated at h_0 will be represented with a subscript of 0; for example,

$$\mathcal{F}'_0 \equiv \mathcal{F}'(h_0). \tag{4.5}$$

We begin by transforming the independent coordinates x, y, z, and t coordinates to X, Y, z, and t coordinates, where $X \equiv x - c_0 t$, $Y \equiv y - d_0 t$, c_0 is defined as

$$c_0 = \mathcal{F}'(h_0) = \mathcal{F}'_0, \tag{4.6}$$

and d_0 is defined as

$$d_0 = \mathcal{G}'(h_0) = \mathcal{G}'_0. \tag{4.7}$$

This is recognized as a coordinate system moving at a constant velocity with x and y components equal to c_0 and d_0, respectively.

The transform of the partial derivatives in (4.1)-(4.2) are:

$$\frac{\partial}{\partial x} = \left.\frac{\partial}{\partial X}\right|_{Y,t}, \tag{4.8}$$

$$\frac{\partial}{\partial y} = \left.\frac{\partial}{\partial Y}\right|_{X,t}, \tag{4.9}$$

and

$$\frac{\partial}{\partial t} = \left.\frac{\partial}{\partial t}\right|_{X,Y} - c_0\left.\frac{\partial}{\partial X}\right|_{Y,t} - d_0\left.\frac{\partial}{\partial Y}\right|_{X,t}. \tag{4.10}$$

If we apply (4.8)-(4.10) to (4.1) we find

$$h_t + (\mathcal{F}' - c_0)h_X + (\mathcal{G}' - d_0)h_Y = -\frac{\sigma}{3\mu}[(h^3(h_{XXX} + h_{YYX}))_X + (h^3(h_{XXY} + h_{YYY}))_Y]. \tag{4.11}$$

In this new equation, h is taken to be $h(X, Y, t)$ and the subscripts now denote partial derivatives in the X, Y, t space.

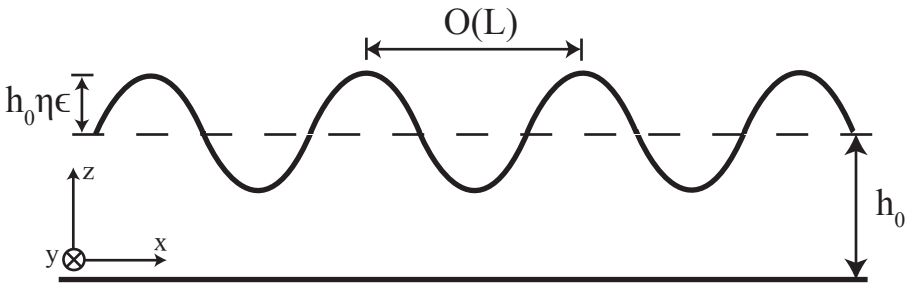

Figure 4.1: Disturbed flow profile, x-z Plane

We will now non-dimensionalize (4.11) using the scalings

$$t = \frac{L}{\Delta c_0}\tau \tag{4.12}$$

$$Y = \frac{L}{\delta}\Upsilon, \tag{4.13}$$

and

$$X = L\chi, \tag{4.14}$$

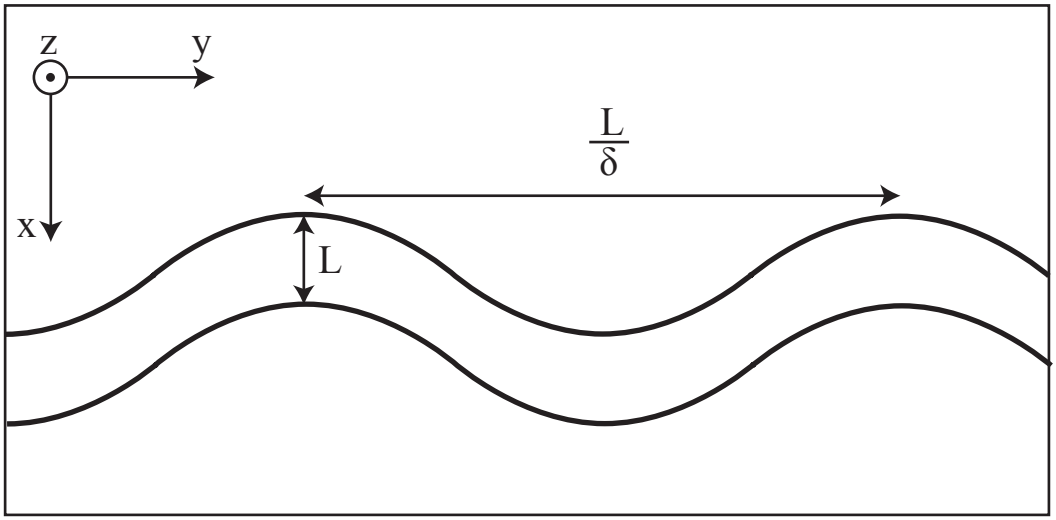

Figure 4.2: Disturbed flow profile, x-y Plane

where L is a measure of the wavelength in the x direction as shown in Figure 4.1, $\frac{L}{\delta}$ is a measure of the wavelength in the y direction as shown in Figure 4.2, and Δ is a non-dimensional measure of the slowness of the wave evolution. For now, Δ and δ are not constrained to be small. If we also take

$$h = h_0(1 + \epsilon\eta), \tag{4.15}$$

as in Figure 4.1 where ϵ is taken to be small, and $\eta = \eta(X, Y, t)$ is the shape of the wave shown in Figure 4.1, we have:

$$\Delta\eta_\tau + \frac{(\mathcal{F}' - c_0)}{c_0}\eta_\chi + \delta\frac{(\mathcal{G}' - d_0)}{d_0}\eta_\Upsilon \approx -Q[\eta\chi\chi\chi\chi + 2\delta^2\eta_{\chi\chi\Upsilon\Upsilon} + \delta^4\eta_{\Upsilon\Upsilon\Upsilon\Upsilon}] + o(Q) \tag{4.16}$$

where $Q \equiv \frac{\sigma h_0^3}{3\mu L^3 c_0}$ is a scaled dissipation coefficient.

A Taylor series expansion of $\mathcal{F}'$ and $\mathcal{G}'$ results in

$$\mathcal{F}' = \mathcal{F}'_0 + \mathcal{F}''_0(h - h_0) + \frac{\mathcal{F}'''_0}{2}(h - h_0)^2 + O(\epsilon^3) \tag{4.17}$$

and

$$\mathcal{G}' = \mathcal{G}'_0 + \mathcal{G}''_0(h - h_0) + O(\epsilon^2). \tag{4.18}$$

If we substitute (4.17) and (4.18) into (4.16) we obtain:

$$\begin{aligned}\Delta\eta_\tau + [h_0\mathcal{F}_0''\epsilon\eta + \frac{\mathcal{F}_0'''h_0^2}{2}\epsilon^2\eta^2 + O(\epsilon^3)]\eta_\chi + \delta[h_0\mathcal{G}_0''\epsilon\eta + O(\epsilon^2)]\eta_\Upsilon \\ \approx -Q[\eta_{\chi\chi\chi\chi} + 2\delta^2\eta_{\chi\chi\Upsilon\Upsilon} + \delta^4\eta_{\Upsilon\Upsilon\Upsilon\Upsilon}] + o(Q).\end{aligned} \tag{4.19}$$

We now examine different limits and approximations to (4.19). These will yield different evolution equations for lowest order value of η.

Chapter 5

Analysis

In the analysis of (4.19) we will examine three distinct cases. In the first case, we will examine linear theory. In this case, we take $\Delta = 1$ so that we are only interested in propagation times which are a few periods of the basic wave. We also take $\epsilon << 1$ and δ is arbitrary. Equation (4.19) then becomes

$$\eta_\tau \approx -Q[\eta_{\chi\chi\chi\chi} + 2\delta^2\eta_{\chi\chi\Upsilon\Upsilon} + \delta^4\eta_{\Upsilon\Upsilon\Upsilon\Upsilon}], \tag{5.1}$$

where Q is not restricted to be any particular size.

Further, if we then restrict $\delta << 1$, (5.1) reduces to

$$\eta_\tau \approx -Q\eta_{\chi\chi\chi\chi}. \tag{5.2}$$

Thus, depending on the initial conditions, we may or may not have to consider transverse dissipation.

In the second case, we will examine quadratically nonlinear behavior. This case corresponds to an undisturbed state that is not near the inflection point of the flux function $\mathcal{F}$. In this case we set $\Delta = \epsilon << 1$, δ is arbitrary, and $Q = O(\epsilon)$. Under these conditions, (4.19) can be seen to be

$$\eta_\tau + h_0\mathcal{F}_0''\eta\eta_\chi + \delta h_0\mathcal{G}_0''\eta\eta_\Upsilon \approx -\frac{Q}{\epsilon}[\eta_{\chi\chi\chi\chi} + 2\delta^2\eta_{\chi\chi\Upsilon\Upsilon} + \delta^4\eta_{\Upsilon\Upsilon\Upsilon\Upsilon}]. \tag{5.3}$$

If the waves are nearly plane, corresponding to $\delta << 1$, then (5.3) reduces to

$$\eta_\tau + h_0\mathcal{F}_0''\eta\eta_\chi \approx -\frac{Q}{\epsilon}\eta_{\chi\chi\chi\chi}. \tag{5.4}$$

Thus, for undisturbed states on most of the $\mathcal{F} - h$ curve, i.e., where $h_0\mathcal{F}_0'' = O(1)$, there is either no influence of the transverse modulations (when $\delta << 1$) or we must retain all three fourth order derivatives in (5.3).

In the third case, we will examine the case where the undisturbed state is in the vicinity of of the inflection point of $\mathcal{F}$. In this case, $h_0\mathcal{F}_0''$ will be small and the system will be locally non-convex. First, two new terms will be defined for convenience,

$$\Gamma \equiv \frac{h_0\mathcal{F}_0''}{\epsilon} \tag{5.5}$$

and

$$\Lambda \equiv h_0^2\mathcal{F}_0''' \tag{5.6}$$

where Γ and Λ will be referred to as the first and second nonlinearity parameters. Near the inflection point $h_0\mathcal{F}_0''$ is small and we will take it to be of order $\epsilon << 1$. Thus we will take $\Gamma = O(1)$ and $\Lambda = O(1)$. Inspection of (4.19) suggests that the nonlinearity will cause variation over nondimensional time scales of order ϵ^{-2}. Thus we will take $\Delta = \epsilon^2$, $Q = O(\epsilon^2)$, and, for now, δ arbitrary. With these choices, (4.19) becomes

$$\eta_\tau + [\Gamma\eta + \frac{\Lambda}{2}\eta^2]\eta_\chi + \frac{\delta}{\epsilon}h_0\mathcal{G}_0''\eta]\eta_\Upsilon \approx -\frac{Q}{\epsilon^2}[\eta_{\chi\chi\chi\chi} + 2\delta^2\eta_{\chi\chi\Upsilon\Upsilon} + \delta^4\eta_{\Upsilon\Upsilon\Upsilon\Upsilon}]. \tag{5.7}$$

To determine the appropriate size for δ we will examine three possiblities. The first possibility is that $\delta << \epsilon$. With δ of this size, the evolution equation becomes

$$\eta_\tau + [\Gamma\eta + \frac{\Lambda}{2}\eta^2]\eta_\chi \approx -\frac{Q}{\epsilon^2}\eta_{\chi\chi\chi\chi}. \tag{5.8}$$

It is seen from (5.8) that the evolution equation in the case of $\delta << \epsilon$ yields the one dimensional equation of [2] and does not retain the derivatives in the transverse direction. That is, when $\delta << \epsilon << 1$, the evolution equation reduces to a non-convex equation which is uninfluenced by transverse modulations.

The second possiblity is that $\delta >> \epsilon$. In this instance, the evolution equation becomes overly trivial and we reject the possibility that $\delta >> \epsilon$. The final possibility is that where $\delta = \epsilon$. With δ of this size, the evolution equation takes the form

$$\eta_\tau + [\Gamma\eta + \frac{\Lambda}{2}\eta^2]\eta_\chi + h_0\mathcal{G}_0''\eta\eta_\Upsilon \approx -\frac{Q}{\epsilon^2}\eta_{\chi\chi\chi\chi}. \tag{5.9}$$

We can see that (5.9) retains the non-convex nonlinearity in the primary direction while also retaining dependence on the transverse direction; this Υ dependence is intrinsically nonlinear.

Chapter 6

Summary

In this thesis we set out to derive from first principles a three dimensional model for the behavior of a thin film flowing on an inclined plane driven by the combined effects of surface tension, Marangoni effect, and gravity. The motivation for the development was to extend the work of [2] to allow for the analysis of the interaction of the nonlinear non-convex convection and fourth order diffusion while retaining the input of effects of the transverse direction of the flow.

To develop the model, we began by making use of the lubication approximations and reduced our fundamental equations. With our reduced funamental equations and boundary equations, we were able to obtain equations for the pressure and velocity of the flow. Making use of the kinematic boundary condition allowed us to find the thin film equation governing the thickness of the film flowing on the incline.

A perturbation analysis of the thin film equation allowed for the developments of an evolution equation for the wavefronts, and subsequent analysis of three different cases for the flow, a linear case, a quadratically nonlinear case, and a non-convex nonlinear case. The nonlinear non-convex case led to an evolution equation depending upon two nonlinearity parameters in the primary direction while retaining effects of the transverse direction.

This evolution equation that has been found will allow for the work of Bertozzi et al [2] to incorporate effects of the transverse flow mdoulation. Further analysis of the undercompressive shocks of [2] is now possible. We believe that the derived equation provides a well defined starting point for future numerical and analytical studies.

Bibliography

[1] J. W. Barrett, J. F. Blowey, and H. Garcke, Finite Element Approximation of a Fourth Order Nonlinear Degenerate Parabolic Equation, Numerische Mathematik, Volume 80, 1998, pp. 525-556.

[2] A. L. Bertozzi, A. Münch, M. Shearer, Undercompressive Shocks in Thin Film Flows, Physica D: Nonlinear Phenomena, Volume 134, Issue 4, 10 December 1999, pp. 431-464.

[3] A. L. Bertozzi and M. Shearer, Existence of Undercompressive Travelling Waves in Thin Film Equations, SIAM Journal on Mathematical Analysis, 2000, pp. 194–213.

[4] B. D. Edmonstone, O.K. Matar, R.V. Craster, Coating of an Inclined Plane in the Presence of Insoluble Surfactant, Journal of Colloid and Interface Science, Volume 287, Issue 1, 1 July 2005, p. 261-272.

[5] X. Fanton,A. M. Cazabat, and, and D. Quéré Thickness and Shape of Films Driven by a Marangoni Flow Langmuir 1996, pp. 5875-5880.

[6] P. D. Lax, Shock Waves and entropy, Contributions to Nonlinear Functional Analysis, Ed. E.H. Zarantonello. Academic Press, 1971.

[7] T. G. Myers, J. P. F. Charpin, and S. J. Chapman, The Flow and Solidification of a Thin Fluid Film on an Arbitrary Three-Dimensional Surface, Physics of Fluids, Volume 14, Issue 8, 2002.

[8] G. A. Naraboli and W. C. Lin, A New Type of Burgers' Equation, ZAMM, Volume 53, 1973, pp. 505-510.

[9] H. Ockendon and J. R. Ockendon, Viscous Flow, Cambridge: Cambridge UP, 1995.

[10] H. H. Saber and M. S. El-Genk, On the Breakup of a Thin Liquid Film Subject to Interfacial Shear, Journal of Fluid Mechanics, Volume 500, April 2004, pp. 113-133.

[11] H. Schlichting, Boundary-Layer Theory, Seventh Edition, New York, McGraw-Hill,1979.

[12] L. W. Schwartz and R. V. Roy, Theoretical and Numerical Results for Spin Coating of Viscous Liquids, Physics of Fluids, Volue 16, Issue 3, pp. 569-584.

Appendix A

Approximation of the Dynamic Boundary Condition

In this appendix we rearrange and approximate (2.7) under the conditions stated in Chapter 2. We begin by writing (2.7) in the following component form:

$$-h_x(P - P_{atm}) - (-h_x T_{xx} - h_y T_{xy} + T_{xz}) = -2\sigma H h_x - (\sigma_x \frac{C}{A} - \sigma_y \frac{h_x h_y}{A}), \tag{A.1}$$

$$-h_y(P - P_{atm}) - (-h_x T_{xy} - h_y T_{yy} + T_{yz}) = -2\sigma H h_y - (\sigma_y \frac{D}{A} - \sigma_x \frac{h_x h_y}{A}), \tag{A.2}$$

$$P - P_{atm} - (-h_x T_{xz} - h_y T_{yz} + T_{zz}) = 2\sigma H - (\sigma_y \frac{h_y}{A} + \sigma_x \frac{h_x}{A}). \tag{A.3}$$

Combining equations (A.1) and (A.3) to eliminate common terms, one can see

$$T_{xz}(1 - h_x^2) - h_x h_y T_{yz} + h_x T_{zz} = h_x T_{xx} + h_y T_{xy} + \sigma_x \frac{C + h_x^2}{A}, \tag{A.4}$$

exactly. We note that

$$T_{xz} = \mu(u_z + w_x) \approx \mu u_z = O\left(\frac{\mu U}{h_0}\right) \tag{A.5}$$

and, in similar manner,

$$T_{yz} = O\left(\frac{\mu U}{h_0}\right). \tag{A.6}$$

The normal stress T_{zz} can be estimated by

$$T_{zz} = 2\mu w_z = O\left(\frac{\mu U}{L}\right) << T_{xz}, T_{yz} \tag{A.7}$$

by (2.26). The normal and shear stresses

$$T_{xx} = 2\mu u_x = O\left(\frac{\mu U}{L}\right) \tag{A.8}$$

$$T_{xy} = 2\mu(u_y + v_x) = O\left(\frac{\mu U}{L}\right). \tag{A.9}$$

Again, by (2.26) we have $T_{xx}, T_{xy} << T_{xz}$. Because T_{yz} in (A.4) is multiplied by

$$h_x h_y = O\left(\frac{h_0^2}{L^2}\right) << 1, \tag{A.10}$$

the largest stress term in (A.4) is the T_{xz} term. Thus,

$$T_{xz} \approx \sigma_x \frac{C + h_x^2}{A} \approx \sigma_x \tag{A.11}$$

on $z = h$ because $A \approx 1$ and $C \approx 1$ for $h_x, h_y << 1$.

If we combine (A.2) and (A.3) a similar analysis will reveal that

$$T_{yz} \approx \sigma_y \tag{A.12}$$

on $z = h$. We can also reduce the stress tensor using the relative sizes of u_x, u_y, u_z etc. When this is done we find:

$$\mathbf{T} \approx \mu \begin{bmatrix} 2u_x & u_y + v_x & \sigma_x \\ u_y + v_x & 2v_y & \sigma_y \\ \sigma_x & \sigma_y & 2w_z \end{bmatrix}. \tag{A.13}$$

Appendix B

Special Cases of Thin Film Equation

In this discussion of the derived model, we will examine several special cases of (3.32). In the first case, we will examine the special case of zero surface tension. The result is

$$h_t + \frac{\rho g \sin(\theta)}{3\mu}(h^3)_x = 0 \tag{B.1}$$

which is a well-known equation governing roll waves [9]. This can be recognized as an inviscid cubic Burgers' equation which also governs one dimensional shear waves in solids and Alfven waves in magnetohydrodynamics [8].

In the second case, all dependence on the transverse flow direction will be removed and we take the surface tension to be constant. The resulting equation is

$$h_t + \frac{\rho g \sin(\theta)}{3\mu}(h^3)_x + \frac{\sigma}{3\mu}(h^3 h_{xxx})_x = 0. \tag{B.2}$$

If the second term in (B.2) is set to zero, the result is the Landau-Levich equation governing surface tension waves in viscous films with constant surface tension (see [9] for derivation). It is seen that one dimensional waves are governed by a combination of a cubic Burgers' equation and the Landau-Levich equation or, equivalently, a cubic Burgers' equation with a fourth order dissipation in place of the classically recognized second order dissipation. In the third special case, we consider the case considered by [2] in which we include the surface tension gradient in the primary direction but continue to ignore effects in the transverse direction. This results in the equation of Bertozzi et al [2]:

$$h_t + \frac{\rho g \sin(\theta)}{3\mu}(h^3)_x + \frac{1}{2\mu}(h^2\sigma_x)_x + \frac{\sigma}{3\mu}(h^3 h_{xxx})_x = 0. \tag{B.3}$$

The nonlinearity of the above equation is now a combined cubic-quadratic nonlinearity. This is often associated with a non-convex flux and can give rise to surprising phenomena. The previous work of Bertozzi et al [2] has been to show the combination of non-convex flux

and fourth order dissipation can give rise to undercompressive shock waves, which appear to violate the Lax speed ordering condition.

In our last example we consider the linearized version of (3.32). If we take $h-h_0$ to be small, the result, to lowest order, is found to be

$$\hat{h}_t + [\frac{\rho g \sin(\theta)}{\mu} h_0^2 + \frac{h_0}{\mu}\sigma_x]\hat{h}_x + \frac{h_0}{\mu}\sigma_y \hat{h}_y + \frac{\sigma}{3\mu} h_0^3 [\hat{h}_{xxxx} + 2\hat{h}_{xxyy} + \hat{h}_{yyyy}] = 0. \tag{B.4}$$

Here $\hat{h} = h - h_0$ is the dimensional perturbation to the constant thickness. We now seek solutions corresponding to plane waves of the form

$$\hat{h} = C_1 e^{i(k_x x + k_y y - \omega t)} \tag{B.5}$$

where $i = (-1)^{1/2}$, ω is the frequency, and k_x and k_y are the x and y are components of the wavenumber vector $\boldsymbol{k}$. Substituting (B.5) into (B.4) we obtain a dispersion relation of the form

$$\omega = [\frac{\rho g \sin(\theta)}{\mu} h_0^2 + \frac{h_0}{\mu}\sigma_x]k_x + \frac{h_0}{\mu}\sigma_y k_y - \frac{i\sigma}{3\mu} h_0^3 k^4, \tag{B.6}$$

where the magnitude of the wave number, k, is defined as

$$k \equiv (k_x^2 + k_y^2)^{1/2}. \tag{B.7}$$

Defining the wave speed as

$$c \equiv \frac{\omega}{k} \tag{B.8}$$

and the unit wave number vector

$$\boldsymbol{\nu} \equiv \frac{\boldsymbol{k}}{k}, \tag{B.9}$$

the dispersion relation can then be rewritten as

$$c = [\frac{\rho g \sin(\theta)}{\mu} h_0^2 + \frac{h_0}{\mu}\sigma_x]\nu_x + \frac{h_0}{\mu}\sigma_y \nu_y - \frac{i\sigma}{3\mu} h_0^3 k^3, \tag{B.10}$$

where ν_x and ν_y are the x and y components of $\boldsymbol{\nu}$. The unit vector $\boldsymbol{\nu}$ can also be shown to be the normal in the the direction of propagation of the planar wave.

From the above dispersion relation, three conclusions can be drawn. First, the system is dissipative with a decay time scale of

$$\frac{3\mu}{\sigma h_0^3 k^4}. \tag{B.11}$$

Second, we observe that the system is dispersive because the wave speed is a function of wavenumber k, both through the dissipative term and through $\boldsymbol{\nu}$. Finally, the system is observed to be anisotropic because the wave speed is a function of the direction of the

propagation, i.e., $\boldsymbol{\nu}$. Another way to conclude that the wave is anisotropic is to compare the wave speeds of waves propagating strictly in the x direction and strictly in the y direction. For example, a wave propagating in purely in the x direction has $\nu_y = 0$, $\nu_x = 1$, and $k = k_x$, thus the wave speed (B.10) reduces to

$$c = \frac{\rho g \sin(\theta)}{\mu} h_0^2 + \frac{h_0}{\mu}\sigma_x - \frac{i\sigma}{3\mu} h_0^3 k^3. \tag{B.12}$$

If the wave is propagating strictly in the y direction, then $\nu_x = 0$, $\nu_y = 1$, and $k = k_y$, yielding

$$c = \frac{h_0}{\mu}\sigma_y - \frac{i\sigma}{3\mu} h_0^3 k^3, \tag{B.13}$$

which is clearly different than the result of waves propagating in the x direction.

If the wave propagation is nearly in the x direction with $\nu_y \approx 0$, $k \approx k_x$ and

$$\nu_x = (1 - \nu_y^2)^{1/2} \approx 1 - \frac{\nu_y^2}{2} + O(\nu_y^4), \tag{B.14}$$

then (B.6) can be written

$$\omega = [\frac{\rho g \sin(\theta)}{\mu} h_0^2 + \frac{h_0}{\mu}\sigma_x]k_x + \frac{h_0}{\mu}\sigma_y k_y - \frac{i\sigma}{3\mu} h_0^3 k_x^4 \tag{B.15}$$

plus higher order terms. The equation governing nearly planar (in the x direction) waves can be recovered from (B.15) by replacing ω by $i\frac{\partial}{\partial t}$, k_x by $-i\frac{\partial}{\partial x}$, k_y by $-i\frac{\partial}{\partial y}$, and k_x^4 by $(-i)^4\frac{\partial^4}{\partial x^4}$. Equation (B.15) can then be shown to be

$$\hat{h}_t + [\frac{\rho g \sin(\theta)}{\mu} h_0^2 + \frac{h_0}{\mu}\sigma_x]\hat{h}_x + \frac{h_0}{\mu}\sigma_y \hat{h}_y + \frac{\sigma}{3\mu} h_0^3 \hat{h}_{xxxx} = 0. \tag{B.16}$$

This is the approximate evolution equation for the the propagation of waves which are nearly in the primary flow direction and is consistent with our final nonlinear equation.

Appendix C

Nonlinearity

To analyze the basic nonlinearity of (3.32) we will begin by ignoring transverse variations and the dissipative term. The resultant equation is

$$h_t + \mathcal{F}_x = 0 \tag{C.1}$$

where the flux in the primary direction, $\mathcal{F}$, is given by

$$\mathcal{F}(h) \equiv \frac{\rho g \sin(\theta)}{3\mu} h^3 + \frac{1}{2\mu}\sigma_x h^2. \tag{C.2}$$

We can also write (C.1) as

$$h_t + \mathcal{F}' h_x = 0 \tag{C.3}$$

where

$$\mathcal{F}' \equiv \frac{d\mathcal{F}}{dh} = \frac{\rho g \sin(\theta)}{\mu} h^2 + \frac{1}{\mu}\sigma_x h \tag{C.4}$$

The exact solution to the Burgers' equation is $h =$ constant on

$$\frac{dx}{dt} = \mathcal{F}'(h). \tag{C.5}$$

We can derive this as follows: if the definition of the total differential is applied to h, the result is

$$dh = h_t dt + h_x dx. \tag{C.6}$$

Dividing by dt leads to

$$\frac{dh}{dt} = h_t + \frac{dx}{dt} h_x \tag{C.7}$$

which is the rate of change of h along a line in $x - t$ space where $x = x(t)$. Requiring that h satisfy the Burgers' equation, the partial derivative h_t can be eliminated leading to

$$\frac{dh}{dt} = (\frac{dx}{dt} - \mathcal{F}')h_x. \tag{C.8}$$

It can be shown that the precise form of h depends upon the initial conditions and for arbitrary initial conditions will remain arbitrary. Thus h is a constant if and only if

$$\frac{dx}{dt} = \mathcal{F}'(h). \tag{C.9}$$

Thus we have proven (C.5). The technique used to prove this is a simplified version of the method of characteristics. The lines defined by (C.5) or (C.9) are called characteristic lines. Recalling that $\mathcal{F}'$ is only a function of h and has no x dependence, $\mathcal{F}'$ is also constant on the characteristic lines. We can obtain the explicit solution by a simple integration to find $h = constant$ on

$$x = constant + \mathcal{F}'t. \tag{C.10}$$

We will now make the claim that for positive values of σ_x the flux function $\mathcal{F}$ both increases as h increases such that $\mathcal{F}' > 0$ and has no inflection points such that $\mathcal{F}'' > 0$ for all values of h. A plot of the behavior of $\mathcal{F}$ is given in Figure C.1. The proof for our claim is easy to see through differentiation of $\mathcal{F}(h)$.

The flux shows that the wave speed increases as h increases; this corresponds to the top of the wave moving faster than the bottom of the wave. The waves will steepen until the characteristic lines cross in the x-t plane and h becomes triple-valued. It is also easily shown that if the surface tension gradient is less than zero and h is greater than zero we can see the flux is negative for $0 < h < 3h_c$ and positive for $h > 3h_c$. We can also see $\mathcal{F}' > 0$ for $h > 2h_c$ and $\mathcal{F}' < 0$ for $0 < h < 2h_c$. Finally, we can also see that $\mathcal{F}'' > 0$ for $h > h_c$ and $\mathcal{F}'' < 0$ for $0 < h < h_c$. In these assertions we shall define h_c as the value of $\mathcal{F}$ at the inflection point of $\mathcal{F}$, i.e. $\mathcal{F}''(h_c) = 0$. Thus

$$h_c \equiv \frac{|\sigma_x|}{2\rho g \sin(\theta)}. \tag{C.11}$$

As before, the proof of this assertion is easily obtained by examining the derivatives of $\mathcal{F}$. The presence of the inflection point causes the curve of $\mathcal{F}$ vs h to be non-convex, in that we can always find a straight line connecting two points on the curve which will intersect the curve at a third location. In the previous case with a positive surface tension gradient, no inflection point was present and the $\mathcal{F}$ vs h curve is referred to as convex. Applying this analysis to the model of this thesis, we will now refer to a system as being either convex or non-convex depending on the nature of the flux function.

As the waves steepen, the leading edge of the wave eventually curls over and becomes triple-valued. Once this occurs, modeling of the wave is accomplished with a discontinuity replacing the triple-valued region; this discontinuity will referred to as a shock or shock wave. To examine the behavior of the shock front, we will ignore the flow in the transverse direction and examine the propagation subject to the non-convex flux and the second and fourth order dissipation. Equation (C.1), with either a second or fourth order dissipation is

$$h_t + \mathcal{F}_x = -\zeta \frac{d^n h}{dx^n} \tag{C.12}$$

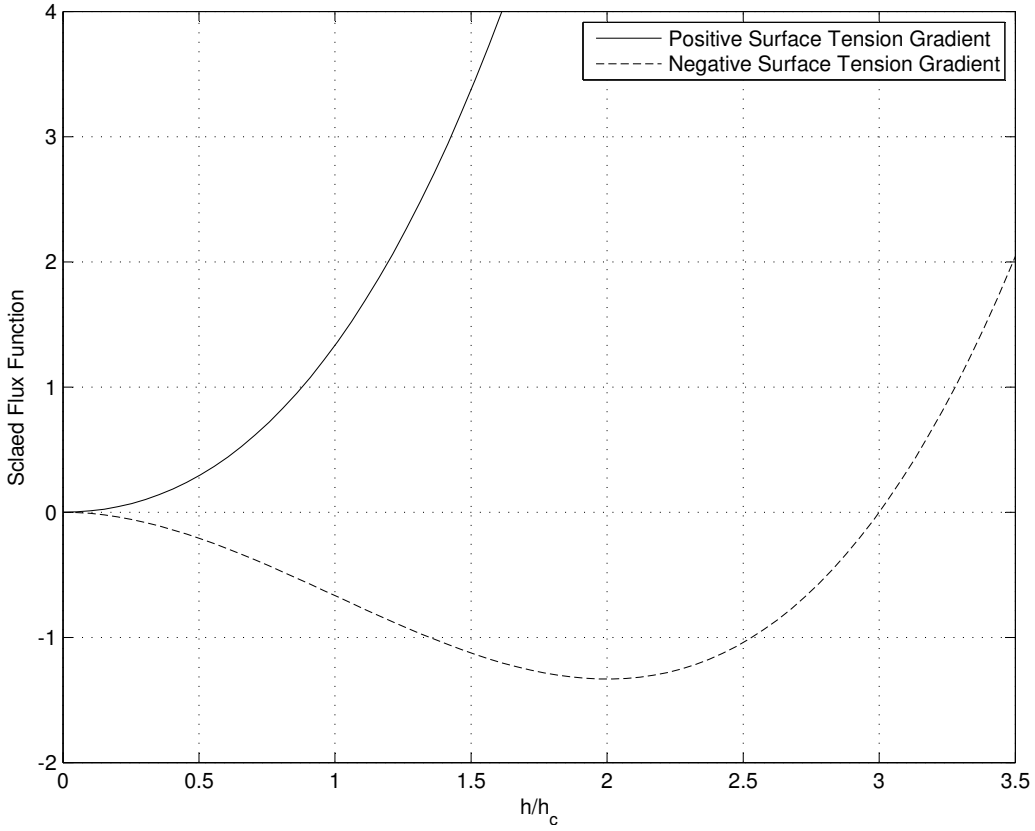

Figure C.1: Plot of the scaled flux function for $\sigma_x > 0$ and $\sigma_x < 0$. The scale factor h_c is the value of h at the inflection point of the non-convex flux.

where n is equal to 2 or 4, depending on the nature of the dissipation, and ζ is a small dissipation parameter. To fully examine the behavior of the shock front, a coordinate transform will be applied. We will replace the current x, and t coordinates with X, y, z, and t coordinates where $X = x - St$. The constant coefficient S is the shock speed. Derivatives in our new coordinate system become

$$\left.\frac{\partial}{\partial x}\right|_t = \left.\frac{\partial}{\partial X}\right|_t, \tag{C.13}$$

and

$$\left.\frac{\partial}{\partial t}\right|_x = \left.\frac{\partial}{\partial t}\right|_X - S\left.\frac{\partial}{\partial X}\right|_t. \tag{C.14}$$

Applying this transform to (C.12) results in

$$h_t + (\mathcal{F} - Sh)_X = -\zeta \frac{d^n h}{dX^n}, \tag{C.15}$$

where the t derivative is taken holding X constant. We now consider "stationary solutions" to (C.15), i.e., those which are independent of time in the X, t coordinates. Thus we will take $h_t = 0$ in (C.15).

A single integration of the resultant equation yields

$$(\mathcal{F} - Sh) = -\zeta \frac{d^{n-1}h}{dX^{n-1}} + k. \tag{C.16}$$

where k is a constant of integration. As $x \to \pm\infty$, h approaches $h^{\pm}$ where $h^{\pm}$ are the values of h far from the shock front. Applying these boundary conditions,

$$k = \mathcal{F}^- - Sh^- \tag{C.17}$$

and

$$k = \mathcal{F}^+ - Sh^+ \tag{C.18}$$

where the superscript denotes the values of $\mathcal{F}$ and h as $x \to \pm\infty$. Substituting for k it can be seen that

$$\mathcal{F}^- - Sh^- = \mathcal{F}^+ - Sh^+. \tag{C.19}$$

Thus, the shock speed S is seen to be

$$S = \frac{\mathcal{F}^+ - \mathcal{F}^-}{h^+ - h^-}. \tag{C.20}$$

When we substitute (C.17) into (C.16) we obtain:

$$\frac{d^{n-1}h}{dX^{n-1}} = -\frac{1}{\zeta}[\mathcal{F} - \mathcal{F}^- - S(h - h^-)]. \tag{C.21}$$

We will now define a Rayleigh line

$$\mathcal{F}_R = \mathcal{F}_R(h) = \mathcal{F}^- + S(h - h^-) \tag{C.22}$$

as a straight line connecting two values of the flux as sketched in Figure C.2. If we substitute (C.22) into (C.21) we have

$$\frac{d^{n-1}h}{dX^{n-1}} = -\frac{1}{\zeta}(\mathcal{F} - \mathcal{F}_R). \tag{C.23}$$

We now consider the case of a second order diffusion. Thus we will take $n = 2$ and $\zeta < 0$ and (C.23) becomes,

$$\frac{dh}{dX} = -\frac{1}{\zeta}(\mathcal{F} - \mathcal{F}_R). \tag{C.24}$$

We will now examine several different Rayleigh lines in the current flow. In the first case we will examine a Rayleigh line connecting two points on the flux function as shown in Figure C.2.

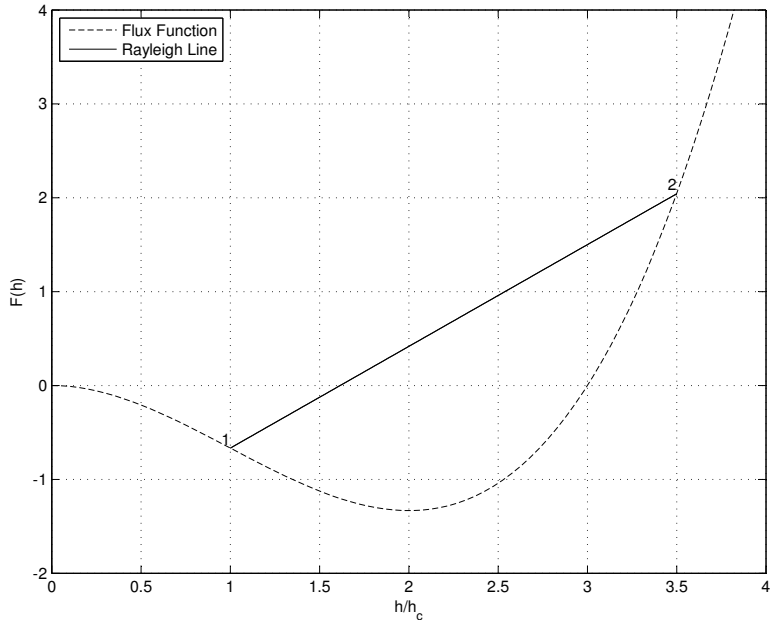

Figure C.2: Plot of non-convex flux with Rayleigh line where $\mathcal{F} < \mathcal{F}_R$ at all $h\epsilon(h_1, h_2)$.

It can be seen that the Rayleigh line $\mathcal{F}_R$ is greater than $\mathcal{F}$. With this in mind, (C.24) requires that $\frac{dh}{dX} < 0$ at every point between the upstream and downstream asymptotes. A representation of h between points 1 and 2 with respect to X is given in Figure C.3. Thus, if the shock is traveling to the right, it results in an increase in h as it passes.

An examination of the slope of the flux function shown in Figure C.2 reveals that

$$\mathcal{F}_2' > S > \mathcal{F}_1' \tag{C.25}$$

meaning that the speed of the flow behind the shock is greater than the speed of the shock which in turn is greater than the speed of the flow ahead of the shock. This is called a compressive shock in [2].

We will examine a Rayleigh line connecting the two different points of the flux as shown in Figure C.4. It can be seen that the Rayleigh line $\mathcal{F}_R$ is less than the flux. With this in mind, (C.24) reveals that $\frac{dh}{dX} > 0$ between the points. A representation of h between points 1 and 2 with respect to X is given in Figure C.5. Thus, a right runnng shock will result in a decrease in h as it passes.

In this case, an examination of the slope of the flux reveals that

$$\mathcal{F}_2' < S < \mathcal{F}_1' \tag{C.26}$$

which is also a compressive shock.

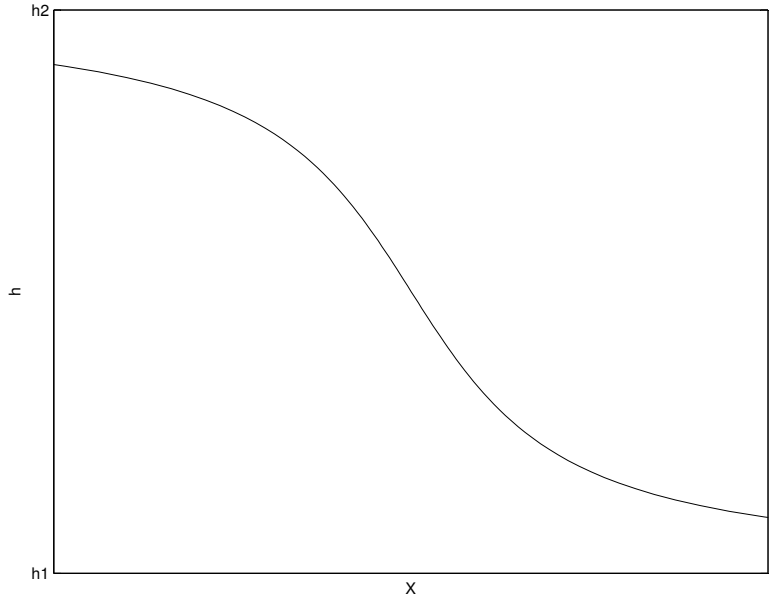

Figure C.3: Plot of h with respect to X, corresponding to Figure C.2.

In the final case we will examine a Rayleigh line as shown in Figure C.6. It can be seen that the Rayleigh line $\mathcal{F}_R$ is less than $\mathcal{F}$ between point 1 and point 3, and greater than $\mathcal{F}$ between point 3 and point 2. With this in mind, (C.24) reveals that $\frac{dh}{dX} < 0$ between the points 1 and 3, and $\frac{dh}{dX} > 0$ between point 3 and 2. A representation of h between points 1 and 2 with respect to X is given in Figure C.7. The plot reveals that there is no acceptable path between points 1 and 2 and this is an inadmissible shock.

Further examination of the relative slopes of the Rayleigh line and the flux function now reveals that

$$\mathcal{F}_2' > S \tag{C.27}$$

and

$$\mathcal{F}_1' > S. \tag{C.28}$$

The waves ahead of the discontinuity in h outpace the shock front and a gap is allowed to develop. In the case of purely second order dissipation, the shock will disintigrate into a smooth wave combined with a shock (private communication with Dr. Cramer).

If we now examine the case in which the fourth order dissipation is dominant, $n = 4$, we can see that

$$h_{XXX} = -\frac{1}{\zeta}(\mathcal{F} - \mathcal{F}_R). \tag{C.29}$$

From this eqaution, it can be seen that in that case where the Rayleigh line intersects the flux

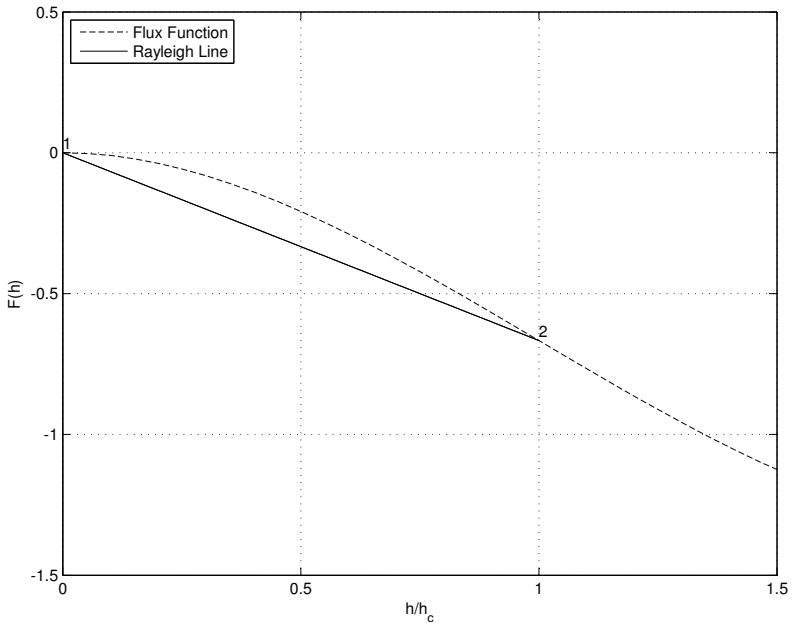

Figure C.4: Plot of non-convex flux with Rayleigh line where $\mathcal{F} > \mathcal{F}_R$ at all $h\epsilon(h_1, h_2)$.

at only two points, the jerk is monotone. It is this case of the interaction of the non-convex flux and the fourth order dissipation that has been of interest to Bertozzi et al in [2], and the simple shock structures seen in the case of the second order dissipation are not possible. The details are contained in [2] and we refer the interested reader there.

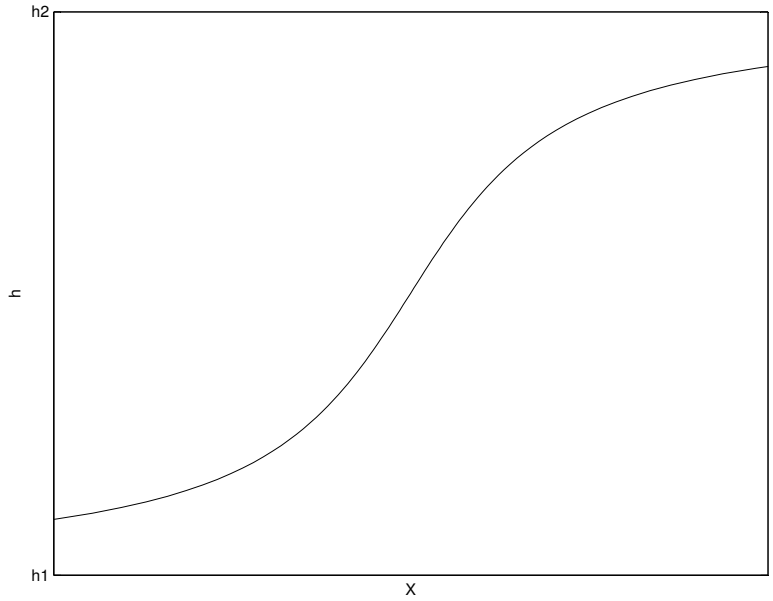

Figure C.5: Plot of h with respect to X, corresponding to Figure C.4.

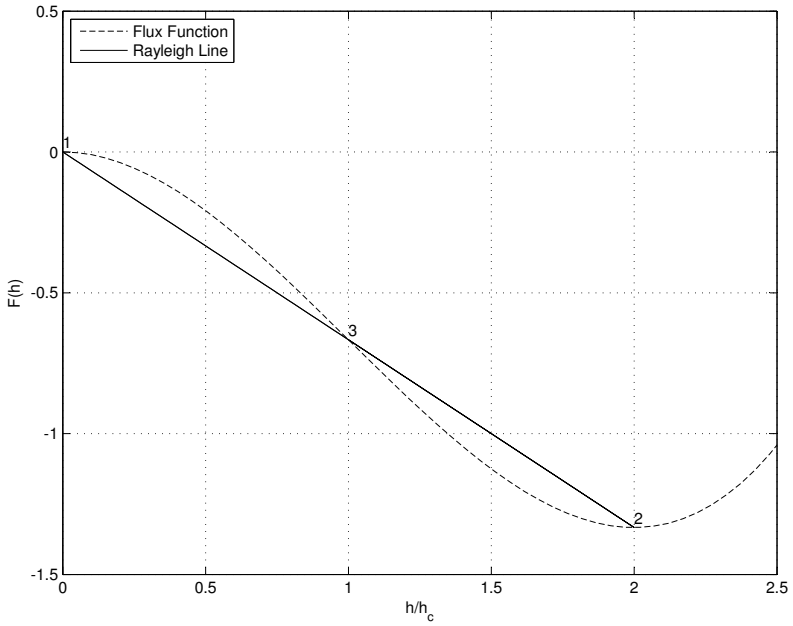

Figure C.6: Plot of non-convex flux with triple intersection Rayleigh line.

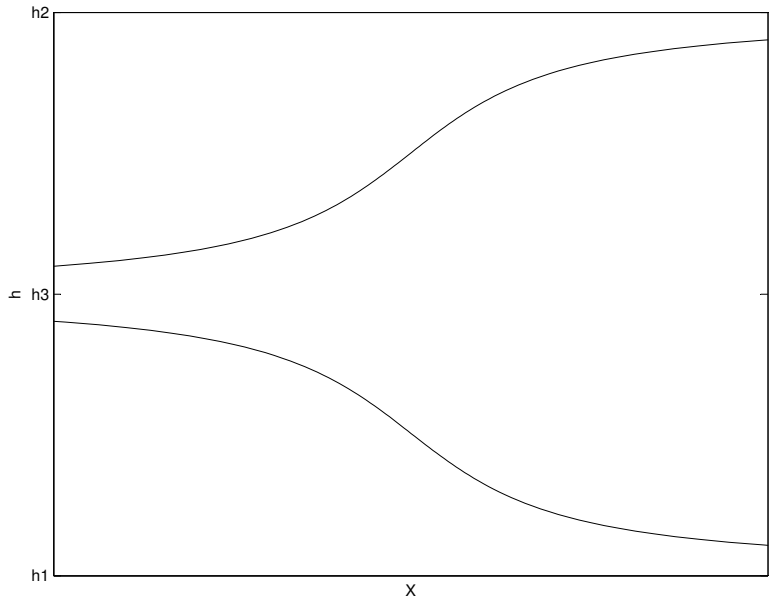

Figure C.7: Plot of h with respect to X, corresponding to Figure C.6.